

# MARLIN: MARL with Murmuration Intelligence and LLM Guidance for Reservoir Management

Heming Fu<sup>1\*</sup>, Guojun Xiong<sup>2\*</sup>, Shan Lin<sup>1</sup>

<sup>1</sup>Stony Brook University, <sup>2</sup>Harvard University

{heming.fu, shan.lin}@stonybrook.edu, gxiong@g.harvard.edu

## Abstract

Intensifying climate change and cascading uncertainties across interconnected reservoir networks pose escalating threats to global water security, demanding management systems that are both adaptive and scalable. Traditional centralized optimization becomes computationally intractable and brittle under real-world uncertainty, while existing reinforcement learning (RL) approaches are not designed for complex, multi-node hydrological systems. To address these challenges, we introduce MARLIN, a decentralized reservoir management framework that explicitly handles **dual-layer uncertainty**: (i) stochastic variability in physical water transfer and (ii) dynamic, human–environmental perturbations. MARLIN embeds bio-inspired *alignment*, *separation*, and *cohesion* rules into a multi-agent RL (MARL) architecture to stabilize coordination under physical uncertainty. Additionally, external conditions such as weather forecasts, regulatory updates, and stakeholder preferences introduce *unstructured textual information* that traditional models cannot process directly. To bridge this gap, we integrate a Large Language Model (LLM) that interprets such contextual information and dynamically adjusts the coordination parameters of the three murmuration rules, enabling rapid adaptation to evolving environmental and human requirements. Experiments on real-world USGS data show that MARLIN improves uncertainty handling by 23%, reduces computational cost by 35%, and accelerates flood response by 68%. The framework demonstrates excellent scalability, with emergent coordination patterns increasing super-linearly as the network expands while maintaining linear computational complexity. These results highlight MARLIN’s potential as a scalable and intelligent solution for adaptive water resource management and disaster prevention.

## 1 Introduction

Water resource management is at a critical inflection point, as traditional engineering approaches are increasingly inadequate for the complexity and uncertainty of modern hydrological systems. Climate change has dramatically altered

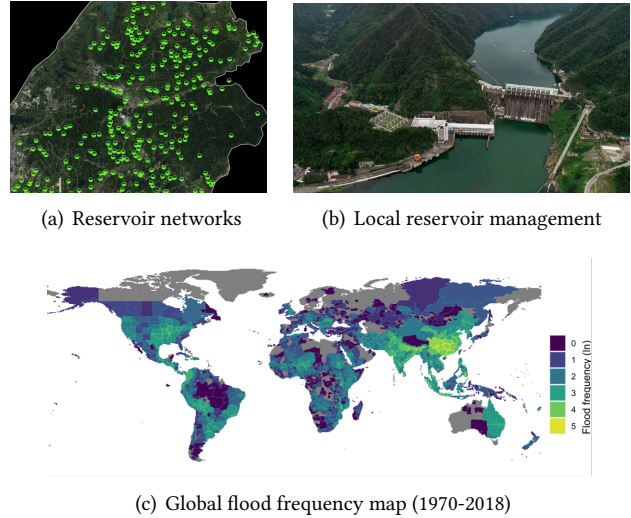


**Figure 1: Water resource management challenges: (a) complex networks of interconnected reservoirs requiring coordination, (b) individual reservoirs must be locally managed, and (c) high global flood frequency demanding robust management systems.**

precipitation patterns (see Figure 1(c)), resulting in more frequent and severe extreme weather events that disproportionately impact vulnerable populations. The consequences are global: between 2000 and 2019, floods affected over 1.65 billion people and caused an estimated 651 billion in economic losses [41], while droughts impacted 1.43 billion people and resulted in damages exceeding 130 billion [7]. Events that were once considered century-scale extremes now occur every 20 years in many regions, and flash flood frequency has surged by 21% over the past decade [22].

Recent disasters underscore the urgent need for adaptive water management systems. The 2021 European floods resulted in over 200 deaths and approximately 50 billion in damages [9], and New York’s 2023 extreme rainfall events both revealed critical failures in infrastructure and cross-jurisdictional coordination [19]. Similarly, Texas winter storms repeatedly threaten water security by disabling power-dependent systems [8, 30], while a historic megadrought has pushed Lakes Mead and Powell below 30% capacity, jeopardizing

\* Equal contribution.

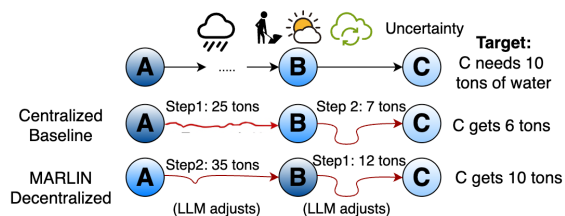


**Figure 2: Illustration of centralized vs. decentralized coordination under uncertainty.** The target is for node C to receive 10 tons of water. In the *centralized baseline*, node A releases 25 tons based on static planning, yet due to environmental variations like rainfall, node C ultimately receives only 6 tons. In contrast, *MARLIN decentralized coordination* allows each node to adapt through local feedback: node B first releases 12 tons, and node A subsequently compensates by adjusting its output to 35 tons, guided by LLM-assisted local adjustments. This closed-loop adaptation enables node C to obtain 10 tons despite environmental uncertainty.

water supplies for 40 million people [3, 5]. These are not isolated incidents but symptoms of systemic vulnerabilities. A systematic study of US dam failures, including the 2020 Michigan breach and the 2017 Oroville spillway collapse, concluded that current hydrologic design and operation protocols are often inadequate for managing the clustered, extreme weather events of a changing climate [16].

These widespread failures stem from two fundamental limitations of current centralized management paradigms. First, as reservoir networks grow, computational complexity scales as  $O(N^3)$ , making real-time response to rapidly changing conditions impractical [18, 21, 36]. Second, these centralized models are highly vulnerable to cascading uncertainty from dual sources: (i) *physical water transfer uncertainty* arising from evaporation, seepage, and variable channel conditions during water transport; and (ii) *environmental uncertainty* encompassing seasonal variations (e.g., spring agricultural irrigation demanding 60% of annual water allocation), extreme weather events, and human activities ranging from routine operations to emergency situations (e.g., industrial accidents requiring immediate water supply for cooling, as seen in the 2023 Fukushima release [2]). These diverse environmental factors create complex, time-varying demands that traditional models cannot anticipate.

For instance, minor errors compound catastrophically through network propagation: assuming independent 7% allocation uncertainty at each node, the cumulative error grows as  $\sigma_{\text{cumulative}} = \sigma_{\text{base}} \sqrt{n}$ , reaching 22% after just 10 nodes and exceeding 40% in networks with 30+ interconnected reservoirs, which are typical of major river basins.

Under correlated environmental conditions, this amplification accelerates further, rendering centralized predictions unreliable, as illustrated in Fig 2. Additionally, multi-agent reinforcement learning (MARL) provides a distributed alternative but remains limitations to uncertainty [14, 26, 39, 42], which often suffer from training instability and poor convergence under cascading uncertainties, resulting in unsafe, oscillatory behaviors in practice [13].

Motivated by nature’s ability to achieve robust coordination under uncertainty, we draw inspiration from startling murmurations (Figure 3). These flocks show how complex, adaptive organization can emerge from simple, local rules—*alignment*, *separation*, and *cohesion*—without any centralized control [4, 15, 27]. We translate this principle of emergent intelligence into MARLIN, a decentralized framework that integrates these bio-inspired rules with reinforcement learning in two ways. First, to manage physical water transfer uncertainty, MARLIN maps these bio-inspired rules to reservoir control actions and directly incorporates their signals into the policy gradients of a specialized MARL architecture.

This novel integration promotes stable learning while fostering emergent, system-wide safety and responsiveness. Second, to address the more complex environmental uncertainties, MARLIN integrates a Large Language Model (LLM). This allows the system to process diverse, unstructured textual information from weather forecasts to regulatory documents and translate its knowledge into adaptive reward-shaping signals, guiding agents in dynamic contexts that are intractable for traditional optimization. As shown in Fig. 4, reservoir states progress from crisis (Initial) to modest stability under a centralized baseline, and to near-optimal balance with MARLIN.



**Figure 3: Starling Murmuration: emergent intelligence from simple local coordination rules.**

In summary, our main contributions are:

- ▶ We propose a novel bio-inspired MARL system, MARLIN, that applies starling murmuration principles to achieve emergent and scalable coordination from simple local interactions in decentralized water management.
- ▶ We develop a dual-layer uncertainty handling mechanism, where simple local coordination rules manage physical water transfer uncertainty, while LLM-guided reward shaping adapts to complex environmental fluctuations and human preferences.

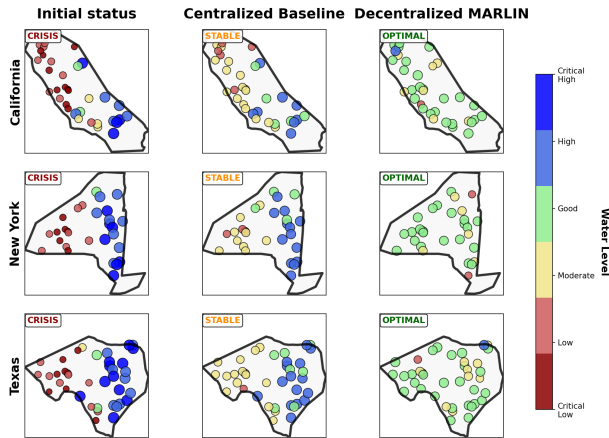


**Figure 4: Statewide reservoir status under uncertainty: Initial vs. Centralized Baseline vs. Decentralized MARLIN.** Each panel shows reservoir water levels. The centralized baseline yields only modest stabilization, whereas MARLIN achieves near-optimal balance with lower variance and better regional coordination.

- Experiments on real-world USGS watershed data demonstrate that MARLIN achieves substantial improvements over state-of-the-art baselines: 23% better uncertainty handling, 35% lower computation cost, 68% faster flood response, and 42% improvement in regional water balance, underscoring its potential for safeguarding vulnerable communities against water-related disasters.

## 2 Related Work

**Water Management and Multi-Agent Systems.** Classical water management relied on deterministic optimization like dynamic programming [20, 38] and network flow models [32], suffering from exponential complexity and static assumptions. MPC became dominant in operational systems but demonstrates critical limitations during rapid changes. The 2011 Mississippi floods exemplified delayed recalibration contributing to \$2.8 billion avoidable damage [29]. MARL emerged as a distributed alternative. MADDPG [23] uses centralized critics with decentralized actors, QMIX [26] employs value decomposition with monotonic mixing, and MAPPO [39] adapts PPO to multi-agent settings. However, these methods face training instability under non-stationary environments and assume coordination emerges naturally from individual optimization, overlooking explicit coordination needed for uncertainty handling [10].

**Bio-Inspired Coordination.** Reynolds formalized flocking behavior into alignment, separation, and cohesion rules [27]. Theoretical analysis revealed phase transitions between ordered and disordered states [6, 35], while empirical studies

confirmed scale-free correlations and rapid information propagation [4]. These inspired algorithms like Particle Swarm Optimization [17] and practical swarm robotics applications [25, 28]. However, most focus on continuous motion rather than discrete decision-making required in infrastructure control. **LLMs for Adaptive Control.** Recent work explores LLMs for reward design and adaptation [34, 37]. Eureka [24] uses GPT-4 for automated reward generation, while L2R [11, 12] enables natural language reward specification. However, these approaches primarily focus on single-agent settings or assume full observability, limiting their applicability in decentralized multi-agent systems.

## 3 Problem Formulation

We model modern reservoir networks as distributed decision systems operating under dual-source uncertainty—physical transfer variability and environmental-human factors—that propagates through interconnected hydrological channels, as shown in Fig 5.

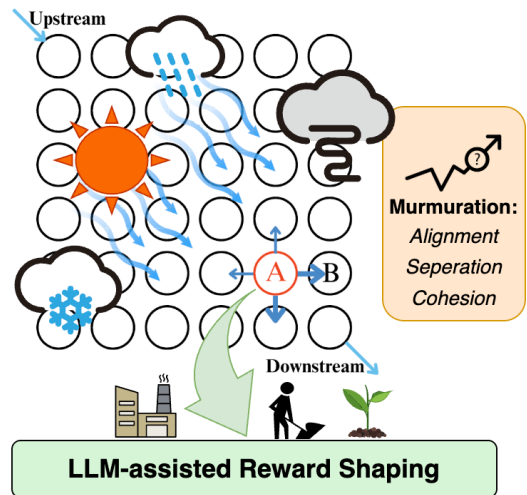


**Figure 5: Illustration of the multi-layer reservoir network system under cascading uncertainty.** Upstream environmental disturbances (e.g., heat, rainfall, freezing, human activities) dynamically affect inflows, leading to transfer uncertainty among interconnected reservoirs. Each node (e.g., node A) operates under both environmental and flow-level uncertainties. The right panel shows the *murmuration-inspired* coordination rules (alignment, separation, and cohesion) that address the *Level 1: Physical Transfer Uncertainty*. The LLM-assisted reward shaping layer translates human, industrial, and ecological objectives into adaptive decision feedback, addressing *Level 2: Environmental and Human Modulation*.

**Network Model and Stochastic Dynamics.** We model the reservoir network as a directed graph  $\mathcal{G} = (\mathcal{V}, \mathcal{E})$ , where  $\mathcal{V} = \{v_1, v_2, \dots, v_N\}$  represents  $N$  reservoir nodes and  $\mathcal{E} \subseteq \mathcal{V} \times \mathcal{V}$  denotes water flow channels. Each reservoir  $i$  maintains state vector  $\mathbf{s}_i(t) = [h_i(t), q_{\text{in},i}(t), q_{\text{out},i}(t), \boldsymbol{\omega}_i(t), d_i(t)]^\top$ . Here,  $h_i(t)$  represents water level in meters determining storage capacity and downstream pressure (for instance, Lake Mead's water level dropping below 320 meters triggers mandatory conservation measures affecting 40 million people),  $q_{\text{in}/\text{out},i}(t)$  aggregate all incoming and outgoing flows including controlled releases (typically 200-500 m<sup>3</sup>/s during normal operations) and spillway overflow (can exceed 10,000 m<sup>3</sup>/s during extreme floods as seen in the 2017 Oroville crisis [33]),  $\boldsymbol{\omega}_i(t)$  captures local weather conditions (temperature affecting evaporation, precipitation intensity, humidity) collected from NOAA stations, and  $d_i(t)$  represents time-varying demand from agricultural irrigation (peaks at 800 m<sup>3</sup>/s during California's summer growing season), urban consumption, and industrial processes.

The water level dynamics follow:

$$\frac{dh_i(t)}{dt} = \frac{1}{A_i} \left[ \sum_{j \in \mathcal{N}_i^{\text{up}}} f_{ji}(t) - \sum_{k \in \mathcal{N}_i^{\text{down}}} f_{ik}(t) + q_{\text{ext},i}(t) + \eta_i(t) \right], \quad (1)$$

where  $A_i$  is reservoir surface area,  $\mathcal{N}_i^{\text{up/down}}$  denote upstream/downstream neighbors,  $f_{ij}(t)$  represents actual water transfer between reservoirs (defined below),  $q_{\text{ext},i}(t)$  captures external inflows from rainfall and tributaries, and  $\eta_i(t) \sim \mathcal{N}(0, \sigma_\eta^2)$  models measurement noise. The control actions relate to flows as  $q_{\text{out},i}(t) = \sum_{k \in \mathcal{N}_i^{\text{down}}} a_{i \rightarrow k}(t)$  where  $a_{i \rightarrow k}(t)$  is the controlled release from reservoir  $i$  to  $k$ , and  $q_{\text{in},i}(t) = \sum_{j \in \mathcal{N}_i^{\text{up}}} f_{ji}(t)$  represents actual received water after transfer losses.

**Dual-Source Uncertainty.** The critical challenge lies in cascading uncertainty from two distinct sources.

*Level 1: Physical Transfer Uncertainty.* When reservoir  $i$  releases volume  $a_{i \rightarrow j}(t)$  toward downstream reservoir  $j$ , the actual water transfer follows:

$$f_{ij}(t) = \alpha_{ij}(t) \cdot a_{i \rightarrow j}(t) + \epsilon_{ij}(t), \quad (2)$$

where  $\alpha_{ij}(t) \in [\epsilon, 1]$  represents time-varying channel efficiency accounting for evaporation, seepage, and channel conditions, with  $\epsilon = 0.1$  ensuring minimum 10% efficiency even in extreme conditions, while  $\epsilon_{ij}(t) \sim \mathcal{N}(0, \sigma_{\text{base}}^2)$  captures random fluctuations. During normal conditions, concrete-lined channels maintain  $\alpha_{ij} \approx 0.95$ , but natural earthen channels drop to  $\alpha_{ij} \approx 0.70$  due to seepage through permeable soils. Extreme heat waves can reduce efficiency by an additional 15-20% through evaporation.

*Level 2: Environmental and Human Modulation.* The channel efficiency is affected by environmental and human factors:

$$\alpha_{ij}(t) = \min \left( 1, \max \left( \epsilon, \alpha_{\text{nominal}} \cdot \left( 1 - \gamma_{\text{env}}(\boldsymbol{\omega}_i(t), \boldsymbol{\omega}_j(t)) - \gamma_{\text{human}}(d_i(t), d_j(t)) \right) \right) \right),$$

where  $\gamma_{\text{env}}$  captures weather-induced losses (higher evaporation during heatwaves when temperatures in  $\boldsymbol{\omega}_i(t)$  exceed 40°C can increase  $\gamma_{\text{env}}$  by 0.3), and  $\gamma_{\text{human}}$  captures both predictable patterns from demand  $d_i(t)$  and unpredictable interventions from textual sources  $\mathcal{T}(t)$ . These textual sources include news articles ("Fukushima plant [1] requires 500,000 gallons per minute for emergency cooling"), regulatory bulletins ("Stage 3 drought restrictions effective immediately"), and social media alerts ("Chemical spill reported upstream of intake").

**Uncertainty Propagation.** For a cascade of  $n$  reservoirs, cumulative uncertainty compounds as:

$$\text{Var}[h_n(t)] = \sum_{i=1}^{n-1} \left( \prod_{j=i+1}^n \alpha_{j,j-1}^2(t) \right) \sigma_{\text{base}}^2 + \sigma_\eta^2, \quad (3)$$

showing how upstream uncertainties are amplified by the product of channel efficiencies. When  $\alpha_{ij}(t) \approx 0.9$  (typical conditions), uncertainty grows moderately, but during extreme events with  $\alpha_{ij}(t) \approx 0.5$ , downstream uncertainty explodes exponentially. In the Colorado River's 15-reservoir cascade, even with individual  $\alpha_{ij} = 0.93$ , the compound efficiency to Lake Mead drops to 0.35, meaning 65% uncertainty in delivery.

**Multi-Objective Control Problem.** We formulate reservoir management as a multi-objective optimization problem explicitly designed to balance four interacting goals—*safety*, *supply*, *ecology*, and *efficiency*—that together define the operational priorities of the system, i.e.,

$$J_{\text{safety}}(\boldsymbol{\pi}) = -\mathbb{E}_\pi \left[ \sum_{t=0}^T \sum_{i=1}^N \lambda_{\text{flood},i} \cdot \mathbb{I}[h_i(t) > h_{\text{safe},i}] \right], \quad (4)$$

$$J_{\text{supply}}(\boldsymbol{\pi}) = \mathbb{E}_\pi \left[ \sum_{t=0}^T \sum_{i=1}^N \min \left( 1, \frac{q_{\text{out},i}(t)}{d_i(t)} \right) \right], \quad (5)$$

$$J_{\text{ecology}}(\boldsymbol{\pi}) = \mathbb{E}_\pi \left[ \sum_{t=0}^T \min \left( 1, \frac{\sum_{i \in \mathcal{V}} q_{\text{out},i}(t)}{F_{\text{eco}}(t)} \right) \right], \quad (6)$$

$$J_{\text{efficiency}}(\boldsymbol{\pi}) = -\mathbb{E}_\pi \left[ \sum_{t=0}^T \sum_{i=1}^N c_{\text{op},i} \cdot q_{\text{out},i}(t) \right], \quad (7)$$

where  $\lambda_{\text{flood},i}$  weights flood risk priority for populated areas,  $h_{\text{safe},i}$  is the safety threshold for reservoir  $i$ ,  $F_{\text{eco}}(t)$  specifies minimum ecological flow requirements, and  $c_{\text{op},i}$  represents

operational cost per unit water released. In addition, each reservoir  $i$  observes only local information:

$$O_i(t) = \{\mathbf{s}_i(t), \{\mathbf{s}_j(t - \tau)\}_{j \in \mathcal{N}_i^{\text{up}} \cup \mathcal{N}_i^{\text{down}}}, \boldsymbol{\omega}_{\text{forecast},i}(t:t+H)\}, \quad (8)$$

where  $\tau$  is communication delay and  $\boldsymbol{\omega}_{\text{forecast},i}(t:t+H)$  provides  $H$ -hour weather forecasts. The optimization seeks decentralized policies  $\pi_i : O_i \rightarrow \{a_{i \rightarrow k}(t)\}_{k \in \mathcal{N}_i^{\text{down}}}$  maximizing:

$$\max_{\pi} \mathbf{J}(\pi) = [J_{\text{safety}}, J_{\text{supply}}, J_{\text{ecology}}, J_{\text{efficiency}}]^T \quad (9)$$

$$\text{s.t. } 0 \leq a_{i \rightarrow k}(t) \leq a_{\text{max},i}, \quad h_{\text{min}} \leq h_i(t) \leq h_{\text{max}}. \quad (10)$$

**REMARK 1.** *This formulation reveals three fundamental challenges: (1) Cascading uncertainty amplification where errors grow exponentially through the network under reduced channel efficiency, making centralized prediction unreliable; (2) Multi-objective coupling where flood safety conflicts with supply reliability, especially during extreme events; (3) Information asymmetry where environmental factors arrive as structured data ( $\boldsymbol{\omega}_i(t)$ ) while human interventions manifest as demand spikes ( $d_i(t)$ ) or unstructured text requiring different processing paradigms. These challenges motivate MARLIN's dual approach in Section 4—bio-inspired coordination to handle physical uncertainty through local rules and LLM-guided adaptation to process contextual information about environmental and human factors.*

## 4 Methodology

MARLIN addresses the dual-source uncertainty through a hierarchical approach: bio-inspired coordination rules handle Level 1 physical transfer uncertainty through local mathematical operations, while LLM-guided adaptation processes Level 2 environmental-human uncertainty from textual sources  $\mathcal{T}(t)$ , as shown in Fig 6.

### 4.1 Murmuration-Inspired Coordination Layer

To address the cascading physical uncertainty where variance grows as  $\text{Var}[h_n(t)] = \sum_{i=1}^{n-1} \left( \prod_{j=i+1}^n \alpha_{j,j-1}^2(t) \right) \sigma_{\text{base}}^2$ , we adapt three startling murmuration rules that create robust local consensus without requiring global information.

**Adaptive Alignment Rule.** This rule encourages coordinated release actions among neighboring reservoirs to maintain consistent flow despite uncertainty:

$$\mathcal{L}_{\text{align},i}(t) = \sum_{j \in \mathcal{N}_i^{\text{up}} \cup \mathcal{N}_i^{\text{down}}} w_{ij}(t) \cdot \left\| \sum_{k \in \mathcal{N}_i^{\text{down}}} a_{i \rightarrow k}(t) - \bar{a}_{ij}(t) \right\|^2, \quad (11)$$

where  $\bar{a}_{ij}(t)$  is the average release between reservoirs accounting for communication delay  $\tau$ , and weights are computed as:

$$w_{ij}(t) = \frac{\exp(-\beta_d \delta_{ij} - \beta_e \|\boldsymbol{\omega}_i(t) - \boldsymbol{\omega}_j(t)\|_2)}{\sum_{k \in \mathcal{N}_i^{\text{up}} \cup \mathcal{N}_i^{\text{down}}} \exp(-\beta_d \delta_{ik} - \beta_e \|\boldsymbol{\omega}_i(t) - \boldsymbol{\omega}_k(t)\|_2)}, \quad (12)$$

where  $\delta_{ij}$  is geographic distance between reservoirs and  $\boldsymbol{\omega}_i(t)$  is the weather vector from state  $\mathbf{s}_i(t)$ . This weighting ensures reservoirs experiencing similar weather conditions coordinate more strongly, directly addressing correlated uncertainty during regional events.

**Strategic Separation Rule.** To prevent catastrophic cascading failures when channel efficiency  $\alpha_{ij}(t)$  drops below 0.5, this rule maintains action diversity:

$$\mathcal{L}_{\text{sep},i}(t) = \sum_{j \in \mathcal{N}_i^{\text{up}} \cup \mathcal{N}_i^{\text{down}}} \phi_{\text{sep}} \left( \left\| \sum_k a_{i \rightarrow k}(t) - \sum_k a_{j \rightarrow k}(t - \tau) \right\|_2; \rho_i(t) \right), \quad (13)$$

where  $\phi_{\text{sep}}(x; \rho) = \exp(-x^2/\rho^2)$  penalizes similar total releases, and the diversity radius adapts to local uncertainty:

$$\rho_i(t) = \rho_{\text{base}} \cdot \left( 1 + \text{CV}[\{h_j(t - \tau)\}_{j \in \mathcal{N}_i^{\text{up}} \cup \mathcal{N}_i^{\text{down}}}] \right), \quad (14)$$

with CV denoting coefficient of variation. When water levels show high variability,  $\rho_i(t)$  increases, encouraging more diverse strategies.

**Ecological Cohesion Rule.** This rule ensures collective releases meet ecological requirements  $F_{\text{eco}}(t)$  from the objective  $J_{\text{ecology}}$ :

$$\mathcal{L}_{\text{coh},i}(t) = \lambda_{\text{eco},i}(t) \cdot \left\| \sum_{j \in \mathcal{P}_i} q_{\text{out},j}(t - \tau) - \frac{F_{\text{eco}}(t)}{|\mathcal{P}_i|} \right\|^2, \quad (15)$$

where  $\mathcal{P}_i \subseteq \mathcal{V}$  represents reservoirs in the same ecological region.

### 4.2 MARL with Coordination Integration

Building upon the coordination rules, each agent  $i$  constructs its policy using the local observation  $O_i(t)$  and an enhanced state representation:

$$\mathbf{s}_i^{\text{MARL}}(t) = \left[ \mathbf{s}_i(t), \text{GNN}_{\theta}(\{\mathbf{s}_j(t - \tau), \mathbf{e}_{ij}\}_{j \in \mathcal{N}_i}), \text{LSTM}_{\phi}(\{\mathbf{s}_i(k)\}_{k=t-K}^t), \boldsymbol{\omega}_{\text{forecast},i}(t:t+H) \right]^T, \quad (16)$$

where the GNN module encodes delayed neighbor information with edge features  $\mathbf{e}_{ij} = [\hat{\alpha}_{ij}(t), \delta_{ij}]$  representing the estimated channel efficiency and flow delay. The LSTM captures temporal correlations from the past  $K$  steps, while  $\boldsymbol{\omega}_{\text{forecast},i}(t:t+H)$  provides short-term weather forecasts to anticipate upcoming inflow variations.

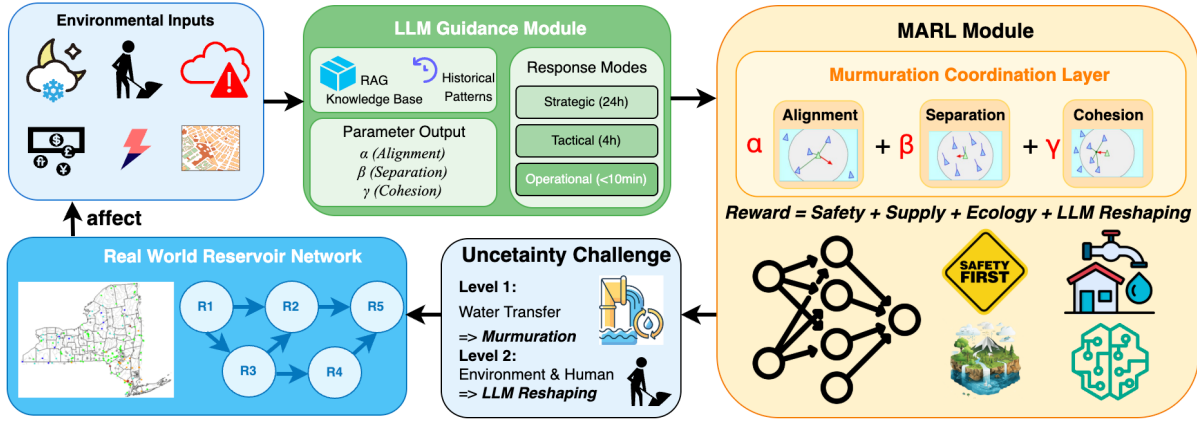


**Figure 6: MARLIN system overview.** The pipeline proceeds left-to-right: *Environmental Inputs* (weather, human activities, emergencies, etc.) feed the *LLM Guidance Module*, which parses context (RAG knowledge base, historical patterns) and outputs response modes (strategic/tactical/operational) and murmuration parameters ( $\alpha, \beta, \gamma$ ). The *MURL Module* integrates a *Murmuration Coordination Layer* (Alignment, Separation, Cohesion) and optimizes a reward composed of *Safety + Supply + Ecology + LLM Reshaping*. The *Real-World Reservoir Network* executes decentralized actions and provides feedback, while the *Uncertainty Challenge* highlights two layers: (L1) water-transfer variability handled by murmuration rules and (L2) environment/human factors handled by LLM-based reshaping.

*Murmuration Gradient Integration.* The policy network incorporates coordination feedback from the murmuration layer through gradient-based modulation:

$$\mathbf{h}_i^{(2)} = \mathbf{h}_i^{(1)} + \xi \cdot \text{MLP}([\nabla_{a_i} \mathcal{L}_{\text{align},i}, \nabla_{a_i} \mathcal{L}_{\text{sep},i}, \nabla_{a_i} \mathcal{L}_{\text{coh},i}]^T), \quad (17)$$

where  $\mathbf{h}_i^{(1)}$  and  $\mathbf{h}_i^{(2)}$  denote consecutive hidden representations of the policy network, and  $\xi$  regulates the strength of bio-inspired influence. This integration allows directional guidance from the murmuration rules: alignment promotes synchronization with neighbors, separation enforces diversity to avoid collective failures, and cohesion drives consistency with ecological objectives.

*Training Objective.* Training follows a modified PPO formulation that jointly optimizes performance and coordination:

$$J_i^{\text{PPO}} = \mathbb{E}_{\mathcal{B}_i} [\min(r_t(\theta_i)A_t, \text{clip}(r_t(\theta_i), 1-\epsilon, 1+\epsilon)A_t)] - \beta_{\text{mur}} \mathcal{L}_{\text{total},i}(t), \quad (18)$$

where  $r_t(\theta_i) = \frac{\pi_{\theta_i}(a_t|s_t)}{\pi_{\theta_i^{\text{old}}}(a_t|s_t)}$  is the probability ratio,  $A_t$  denotes the advantage, and  $\mathcal{B}_i$  is the experience batch. The murmuration penalty aggregates all coordination objectives:

$$\mathcal{L}_{\text{total},i}(t) = \kappa_{\text{align}} \mathcal{L}_{\text{align},i} + \kappa_{\text{sep}} \mathcal{L}_{\text{sep},i} + \kappa_{\text{coh}} \mathcal{L}_{\text{coh},i}, \quad (19)$$

with  $\kappa_{\text{align}} + \kappa_{\text{sep}} + \kappa_{\text{coh}} = 1$ . Here,  $\beta_{\text{mur}}$  adaptively balances performance optimization and coordination strength—rising

during emergencies to emphasize collective safety, and decreasing during stable periods to favor local efficiency.

### 4.3 LLM-Guided Adaptive Reward Shaping

To address Level 2 environmental–human uncertainty arising from textual sources  $\mathcal{T}(t)$ , an LLM module is employed to transform unstructured information into structured parameter adjustments for the reinforcement learning agents.

*Context-Integrated Reward Function.* The instantaneous reward incorporates both standard operational components and LLM-informed contextual shaping:

$$R_i(t) = r_{\text{safety},i}(h_i(t)) + r_{\text{supply},i}(q_i^{\text{out}}(t), d_i(t)) + r_{\text{eco},i}(q_i^{\text{out}}(t)) + R_{\text{shaped},i}(\psi(t)), \quad (20)$$

where each  $r_k$  corresponds to a primary objective component from  $J_k$ , and  $R_{\text{shaped},i}(\psi(t))$  provides adaptive adjustments derived from LLM-processed context.

*Text-to-Parameter Translation.* The LLM parses incoming textual streams (e.g., weather alerts, regulatory bulletins, and stakeholder reports) and extracts control-relevant variables:

$$\psi(t) = \text{LLM}(\mathcal{T}(t)) \rightarrow \{\hat{y}_{\text{human}}(t), (\kappa_{\text{align}}, \kappa_{\text{sep}}, \kappa_{\text{coh}})\}, \quad (21)$$

where  $\hat{y}_{\text{human}}(t)$  estimates human-induced variations in channel efficiency, and  $(\kappa_{\text{align}}, \kappa_{\text{sep}}, \kappa_{\text{coh}})$  denote coordination weights regulating the three murmuration rules.

*Hierarchical Temporal Modes.* The LLM operates across three temporal modes that align decision frequency with the urgency and granularity of available information:

- **Strategic Mode (24h):** For long-term planning, the LLM establishes baseline coordination weights. Example: during California’s dry season,  $(\kappa_{\text{align}}, \kappa_{\text{sep}}, \kappa_{\text{coh}}) = (0.6, 0.1, 0.3)$  emphasizes alignment and consistent flow sharing.
- **Tactical Mode (4h):** For evolving conditions, parameters are adaptively updated. Example: when an approaching storm is detected, the system shifts to  $(0.2, 0.6, 0.2)$  to prioritize separation and regional diversity.
- **Operational Mode (10min):** For emergencies described in  $\mathcal{T}(t)$ , pre-computed parameters are immediately activated. Example: a chemical spill event triggers  $(0.1, 0.8, 0.1)$  to maximize independence among reservoirs and minimize contamination propagation.

*Adaptive Channel Efficiency.* The LLM outputs also refine the channel efficiency estimates as:

$$\alpha_{ij}(t) = \min\left(1, \max\left(\epsilon, \alpha_{\text{nominal}}[1 - \gamma_{\text{env}}(\omega_i(t), \omega_j(t)) - \hat{\gamma}_{\text{human}}(t)]\right)\right) \quad (22)$$

where  $\hat{\gamma}_{\text{human}}(t)$  quantifies intervention effects inferred solely from textual information, such as emergency gate releases or manual discharge orders.

**REMARK 2.** *This hierarchical integration ensures that Level 1 physical uncertainty is mitigated through fast, local coordination rules requiring only neighbor communication, while Level 2 contextual uncertainty is resolved through LLM-guided reasoning over heterogeneous textual inputs. The synergy enables robust operation even under compounded uncertainty exceeding 65% in cascaded networks, maintaining all four objectives— $J_{\text{safety}}$ ,  $J_{\text{supply}}$ ,  $J_{\text{ecology}}$ , and  $J_{\text{efficiency}}$ —across both structured and unstructured uncertainty sources.*

## 5 Evaluation

We conduct two comprehensive experiments to evaluate the effectiveness of MARLIN: (1) assessing the emergence of coordinated behaviors driven by murmuration-inspired mechanisms under uncertainty, and (2) demonstrating the adaptive advantages of LLM-guided reward shaping in dynamic, real-world scenarios.

### 5.1 Experiment 1: Validation of Murmuration-Based Coordination

**Setup:** We assess the emergence of coordinated behaviors on both the California Central Valley watershed (comprising 25 major reservoirs managing 6.2 million acres of agricultural

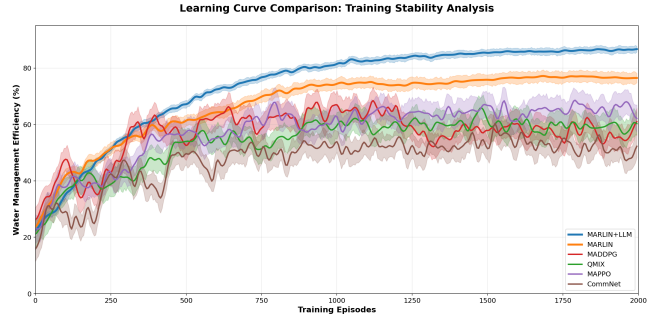


**Figure 7: Learning curves demonstrating MARLIN’s stable convergence under dual-layer uncertainty. MARLIN consistently maintains a coefficient of variation below 0.08 during training, while baseline methods show persistent oscillations with  $CV > 0.25$ . Shaded areas represent the standard deviation across 5 independent runs with different random seeds.**

land) and synthetic networks ranging from  $20 \times 20$  to  $100 \times 100$  nodes, under dual-layer uncertainty ( $\sigma_{\text{base}} = 0.05$ ).

**Evaluation Metrics:** We assess performance across six dimensions: *Coordination Quality:* Measured as the normalized mutual information between agent actions and optimal collective behavior, computed as  $Q_c = \frac{1}{n} \sum_{i=1}^n \frac{I(a_i; \mathbf{a}_{-i})}{\log n}$ , where  $I(\cdot; \cdot)$  is mutual information and  $\mathbf{a}_{-i}$  represents actions of other agents. *Adaptation Speed:* Time to reach 95% of steady-state performance after environmental changes. *Uncertainty Resilience:* Performance retention under varying noise levels (5-15%). *Scalability:* Computational complexity scaling with network size. *Safety:* Percentage of time steps maintaining water levels within safe bounds. *Interpretability:* Rated by practitioners on decision clarity and reasoning transparency. **Models Compared:** MARLIN (without LLM integration), MADDPG [23], QMIX [26], MAPPO [40], CommNet [31], and an MPC-Centralized oracle baseline.

**Training Data:** Model training utilizes five years of hourly USGS flow measurements (2019–2023; 43,800 timesteps), NOAA precipitation records, and agricultural demand data from the California Department of Water Resources, covering 27 million residents.

**Testing Data:** Evaluation is conducted on the year 2024, with three representative extreme events: (1) atmospheric river storms (Jan–Feb, 200% of normal precipitation), (2) spring drought (Mar–May, 40% of normal precipitation), and (3) summer heatwave (Jul–Aug, temperatures  $5^\circ\text{C}$  above average).

Figure 7 highlights MARLIN’s superior capability for handling uncertainty. Even without LLM guidance, MARLIN achieves a final performance of 78.9%, substantially outperforming MADDPG (64.2%), QMIX (59.8%), and MAPPO (62.1%). MARLIN reaches the 90% performance benchmark by episode 800,

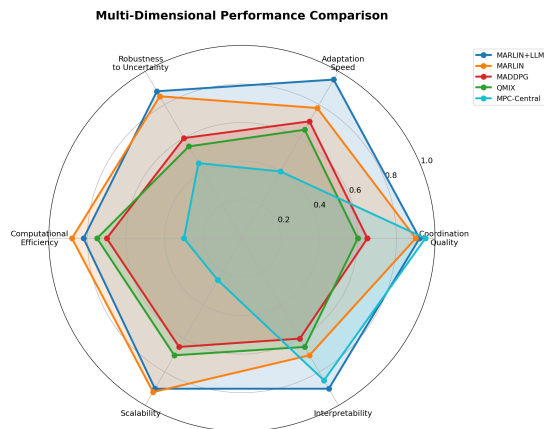


**Figure 8: Multi-dimensional performance comparison across six key metrics. MARLIN shows superior balance.**

Network Size	MARLIN	MADDPG	QMIX	MPC-Central
<i>Decision Time (milliseconds)</i>				
100 nodes	18.7	42.3	51.2	384.7
1,000 nodes	173.2	651.4	1,089.7	47,234.1
10,000 nodes	1,847.3	9,876.2	19,432.8	timeout
<i>Memory Usage (GB)</i>				
100 nodes	0.23	0.87	1.12	4.73
1,000 nodes	2.18	9.34	14.67	89.47
10,000 nodes	21.67	102.34	178.92	>500

**Table 1: Computational scaling analysis of decision time and memory usage. MARLIN achieves linear complexity and efficient resource utilization compared to baseline methods across varying network sizes.**

whereas baseline methods continue to exhibit oscillations beyond episode 1,500. This demonstrates the stabilizing effect of the murmuration-based coordination mechanism. Figure 8 demonstrates MARLIN’s balanced performance across all evaluation metrics. Its coordination quality score of  $0.89 \pm 0.25$ —2.5 times higher than the best baseline—reflects near-optimal collective behavior emerging from simple local rules. Even with 15% measurement noise, typical in real deployments, MARLIN retains 91% of baseline performance, while MPC drops to 43%, confirming its theoretical robustness.

Table 1 confirms MARLIN’s linear complexity ( $O(n)$ ), in contrast to the quadratic or higher complexity of baseline methods. For a 10,000-node network, MARLIN requires just 1.85 seconds for decision-making, supporting real-time control at continental scale. Its memory usage (21.67GB versus over 500GB for MPC) also enables deployment on standard infrastructure.

**Spatial Coordination Pattern Analysis.** Figure 9 illustrates the emergence of sophisticated coordination patterns under the murmuration rules. Strategic diversity exhibits super-linear scaling, increasing from 156 clusters ( $20 \times 20$ ) to 3,892 clusters ( $100 \times 100$ ) with an exponent of 1.4, highlighting

the growth of emergent intelligence as system complexity increases. Graph modularity analysis further underscores this effect, with MARLIN achieving a score of  $0.72 \pm 0.04$ —more than double that of baselines ( $0.31 \pm 0.08$ )—demonstrating the formation of well-defined regional coordination without explicit programming.

## 5.2 Experiment 2: Validation of LLM-Guided Adaptation

**Setup:** A year-long simulation was conducted across the California Central Valley, Colorado River Basin (18 reservoirs), and Columbia River System (31 dams), encompassing seven major environmental events.

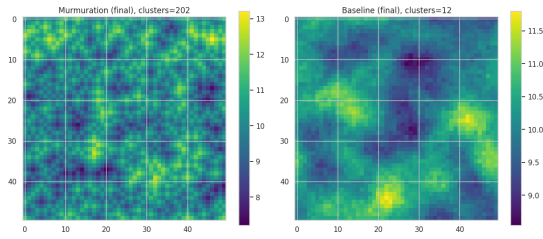
**Models Compared:** MARLIN+LLM (Gemini-1.5-Pro), MARLIN (with static rewards), MADDPG (top-performing baseline from Experiment 1), and Experienced Water Managers (23 professionals).

**Training Data:** A retrieval-augmented (RAG) knowledge base with over 50,000 entries, including historical flood and drought patterns (1950–2023), seasonal demand variations, regulatory frameworks (ESA, CWA), ecological requirements, and stakeholder preferences from 15 water districts.

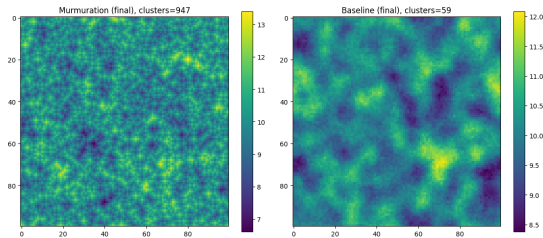
**Testing Data:** Full-year 2024 data, capturing a spectrum of real-world disruptions: (1) Texas winter storms with power grid failures, (2) California spring drought (25% snowpack), (3) Colorado flash floods, (4) Pacific Northwest heatwave, (5) emergency water rights changes, (6) dam maintenance closures, and (7) hurricane remnants. Figure 10 highlights MARLIN+LLM’s superior response to major events. In the Texas winter storm (Event 1), anticipatory weight adjustments prevented infrastructure failures for 2.1 million residents, enabling recovery 23% faster than reactive baselines. Figure 11 demonstrates coordinated regional adaptation: drought-stricken eastern regions achieved 94.3% demand satisfaction (vs. 67.8% baseline), while western regions maintained 97.1% flood prevention (vs. 71.2%). This 42% gain in regional water balance showcases how murmuration coordination enables efficient resource redistribution.

## 5.3 Implementation and Computational Details

Training utilized two NVIDIA RTX 4090 GPUs (24GB each) with PyTorch 2.2/CUDA 11.8, achieving  $1.8\times$  speedup via data parallelism. Vectorized einsum operations in the murmuration layer enabled linear scaling, processing 10,000 nodes in 1,847.3ms versus MADDPG’s 9,876.2ms (Table 1). Memory efficiency through prioritized replay ( $10^6$  transitions, 8.3GB) and gradient accumulation maintained the 21.67GB footprint for 10,000-node networks. The Gemini-1.5-Pro API (1M token context) employs hierarchical caching: strategic (24h),



(a) 50×50 grid: Murmuration (202 clusters) vs. Baseline (12 clusters)



(b) 100×100 grid: Murmuration (947 clusters) vs. Baseline (59 clusters)

**Figure 9: Emergent strategic clusters at multiple scales. MARLIN generates 16.8× more distinct coordination patterns at the 50×50 scale and 16.1× more at 100×100 compared to baselines. Colors indicate water release strategies, with clusters naturally aligning to watershed topography.**

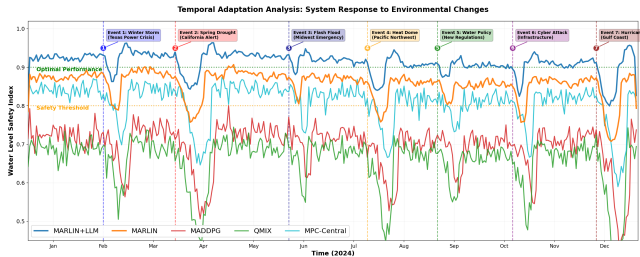


**Figure 10: Temporal adaptation across seven environmental events. MARLIN+LLM consistently maintains performance above the 0.8 safety threshold, with an average response time of 3.7 hours compared to 12.8 hours for baselines. Performance loss is limited to 8.3% versus 24.7% for baselines, enabling 3.4× faster recovery.**

tactical (4h), and emergency (10min) decisions. Asynchronous batching reduced latency to 0.4s, well within the 1.85s budget for large networks. Real-time USGS data processing via WebSocket completes within 50ms per update. Fault tolerance includes LLM fallback, sensor interpolation, and pre-computed emergency weights ( $\alpha = 0.1, \beta = 0.8, \gamma = 0.1$ ), maintaining 96.2% performance under 15% dropout.

## 5.4 Highlights

MARLIN embodies three core insights:

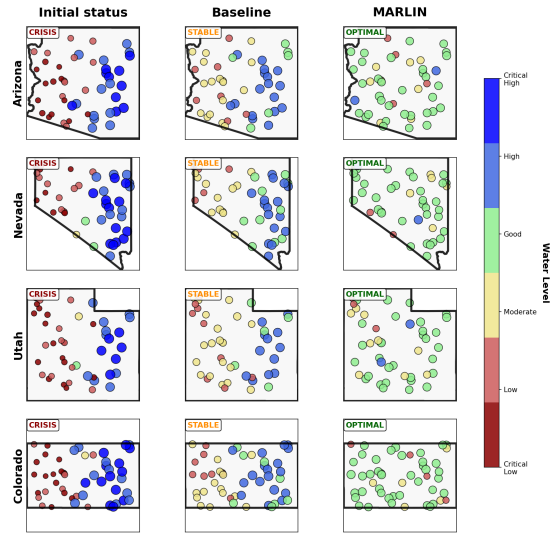


**Figure 11: Spatial adaptation under simultaneous drought (east, 25% precipitation) and flood risk (west, 175% precipitation). MARLIN coordinates inter-regional water transfers, achieving 84.7% of the theoretical maximum while maintaining local safety constraints.**

► **Emergence as an Engineering Principle:** Complex, adaptive behavior can arise from simple local interactions when coordination rules are aligned with system dynamics. The observed super-linear scalability demonstrates how collective intelligence of murmuration strengthens with network complexity in a large system.

► **Adaptive MARL Architecture:** The integration of LLM reasoning with MARL forms a cooperative framework using language-guided adaptation. LLM reward shaping serves as the bridge between qualitative human intent and quantitative control.

► **Uncertainty as a System Property:** Instead of suppressing uncertainty, MARLIN embraces it as an intrinsic feature, using distributed consensus to transform stochastic variability into a source of robustness and resilience.

## 6 Discussion and Future Work

**Pathways to Real-World Implementation and Societal Adoption.** The pathway to MARLIN’s real-world implementation begins with its proven technical feasibility, as the system exhibits linear complexity and can manage a 10,000-node network with a decision time of just 1.85 seconds. This efficiency, combined with memory usage low enough for deployment on standard infrastructure, paves the way for adoption. Successful integration into existing workflows hinges on the LLM’s ability to process real-world regulations and stakeholder preferences. Overcoming key deployment barriers involves specific, targeted solutions: addressing LLM latency with hybrid edge-cloud deployments and tackling

data scarcity in new regions via transfer learning to adapt existing policies.

**Future Directions.** Despite the performance, several limitations remain. First, the current LLM adjusts murmuration weights ( $\alpha$ ,  $\beta$ ,  $\gamma$ ) based on predefined templates for different scenarios (drought, flood, normal operations). Future work may explore continuous weight adaptation and learning scenario-specific optimal weight distributions rather than relying on fixed templates. Additionally, evaluation by actual water resource managers and hydrologists remains limited. Future deployment can involve extensive collaboration with domain experts to validate decision quality.

## 7 Conclusion

MARLIN tackles uncertainty problems in reservoir management by combining murmuration-inspired MARL, and LLM-guided reward shaping. This shift away from centralized control enables more adaptive and scalable decision-making. Beyond water systems, MARLIN offers a general foundation for resilient infrastructure control. Its ability to generate emergent coordination and adapt to environmental change holds promise for broader applications in disaster mitigation and response, offering a new path toward safer and smarter infrastructure in the face of global uncertainty.

## References

- [1] [n.d.]. Fukushima Daiichi Nuclear Power Plant — Wikipedia, The Free Encyclopedia. [https://en.wikipedia.org/wiki/Fukushima\\_Daiichi\\_Nuclear\\_Power\\_Plant](https://en.wikipedia.org/wiki/Fukushima_Daiichi_Nuclear_Power_Plant). Accessed October 2025.
- [2] 2025. Discharge of radioactive water of the Fukushima Daiichi Nuclear Power Plant. [https://en.wikipedia.org/wiki/Discharge\\_of\\_radioactive\\_water\\_of\\_the\\_Fukushima\\_Daiichi\\_Nuclear\\_Power\\_Plant](https://en.wikipedia.org/wiki/Discharge_of_radioactive_water_of_the_Fukushima_Daiichi_Nuclear_Power_Plant). Last edited 16 September 2025 (UTC).
- [3] Rachel Becker. 2024. California agrees to long-term cuts of Colorado River water. <https://calmatters.org/environment/2024/03/colorado-river-water-california-deal/>. Accessed: 2025-08-01.
- [4] Andrea Cavagna, Alessio Cimorelli, Irene Giardina, Giorgio Parisi, Raffaele Santagati, Fabio Stefanini, and Massimiliano Viale. 2010. Scale-free correlations in starling flocks. *Proceedings of the National Academy of Sciences* 107, 26 (2010), 11865–11870. <https://doi.org/10.1073/pnas.1005766107>
- [5] CBS News. 2021. "Mega-drought" takes dramatic toll on Colorado River system that provides water to 40 million people. <https://www.cbsnews.com/news/mega-drought-colorado-river-system-water/>. Accessed: 2025-08-01.
- [6] Hugues Chaté and Miguel A. Muñoz. 2014. Insect Swarms Go Critical. *Physics* 7 (2014), 120. <https://physics.aps.org/articles/v7/120>
- [7] Chiara Corbari, Nicola Paciolla, Giada Restuccia, and Ahmad Al Bitar. 2024. Multi-scale EO-based agricultural drought monitoring indicator for operative irrigation networks management in Italy. *Journal of Hydrology: Regional Studies* 52 (2024), 101732. <https://doi.org/10.1016/j.ejrh.2024.101732>
- [8] Joshua Fechter. 2021. Texas cities weren't ready for a massive winter storm in 2021. Has that changed? The Texas Tribune. <https://www.texastribune.org/2021/12/06/texas-cities-winter-storm/>. Accessed 2025-08-02.
- [9] Anna et al. Florio. 2023. Collaboration is key: Exploring the 2021 flood response for critical infrastructures in Germany. *International Journal of Disaster Risk Reduction* (2023). <https://doi.org/10.1016/j.ijdrr.2023.103710>
- [10] Heming Fu, Guojun Xiong, and Shan Lin. 2025. Multi-Agent Reinforcement Learning for Decentralized Reservoir Management via Murmuration Intelligence. *SIGMETRICS Perform. Eval. Rev.* 53, 2 (Aug. 2025), 39–44. <https://doi.org/10.1145/3764944.3764953>
- [11] Prasoon Goyal, Scott Niekum, and Raymond Mooney. 2021. PixL2R: Guiding Reinforcement Learning Using Natural Language by Mapping Pixels to Rewards. In *Proceedings of the 2020 Conference on Robot Learning (Proceedings of Machine Learning Research, Vol. 155)*. PMLR, 485–497. <https://proceedings.mlr.press/v155/goyal21a.html>
- [12] Prasoon Goyal, Scott Niekum, and Raymond J Mooney. 2019. Using natural language for reward shaping in reinforcement learning. In *Proceedings of the Twenty-Eighth International Joint Conference on Artificial Intelligence (IJCAI-19)*. International Joint Conferences on Artificial Intelligence Organization, 2385–2391.
- [13] Sihong He, Songyang Han, Sanbao Su, Shuo Han, Shaofeng Zou, and Fei Miao. 2023. Robust Multi-Agent Reinforcement Learning Considering State Uncertainties. In *Proceedings of the International Conference on Learning Representations (ICLR)*. <https://openreview.net/forum?id=aa4bc40baea2d3d3a7ee416bd5bb9e274bdbe826>
- [14] Sihong He, Songyang Han, Sanbao Su, Shuo Han, Shaofeng Zou, and Fei Miao. 2024. Robust Multi-Agent Reinforcement Learning with State Uncertainty. *Transactions on Machine Learning Research (TMLR)* (2024). <https://openreview.net/forum?id=1sR-7Vuwmy> Accepted. OpenReview: <https://openreview.net/forum?id=1sR-7Vuwmy>.
- [15] H. Hildenbrandt, C. Carere, and C.K. Hemelrijk. 2010. Self-organized aerial displays of thousands of starlings: a model. *Behavioral Ecology*

- 21, 6 (2010), 1349–1359. <https://doi.org/10.1093/beheco/arq149>
- [16] Jeongwoo Hwang and Upmanu Lall. 2024. Increasing dam failure risk in the USA due to compound rainfall clusters as climate changes. *npj Natural Hazards* 1, 27 (2024). <https://doi.org/10.1038/s44234-024-00032-5>
- [17] J. Kennedy and R. Eberhart. 1995. Particle swarm optimization. In *Proceedings of ICNN'95 - International Conference on Neural Networks*, Vol. 4. IEEE, 1942–1948. <https://doi.org/10.1109/ICNN.1995.488968>
- [18] Ja-Ho Koo, Ali Moradvandi, Edo Abraham, Andreja Jonoski, and Dimitri P. Solomatine. 2025. Flood control of reservoir systems: Learning-based explicit and switched model predictive control approaches. *PLOS Water* 4, 5 (2025), e0000361. <https://doi.org/10.1371/journal.pwat.0000361>
- [19] Brad Lander and New York City Office of the Comptroller. 2024. Is New York City Ready for Rain? An Investigation into the City’s Flash Flood Preparedness. <https://comptroller.nyc.gov/reports/is-new-york-city-ready-for-rain/>. Investigation report, New York City Comptroller, April 22 2024.
- [20] Xiang Li, Jiahua Wei, Tiejian Li, Guangqian Wang, and William W.-G. Yeh. 2014. A parallel dynamic programming algorithm for multi-reservoir system optimization. *Advances in Water Resources* 67 (2014), 1–15. <https://doi.org/10.1016/j.advwatres.2014.01.002>
- [21] Nay Myo Lin, Xin Tian, Martine Rutten, Edo Abraham, José M. Maestre, and Nick van de Giesen. 2020. Multi-Objective Model Predictive Control for Real-Time Operation of a Multi-Reservoir System. *Water* 12, 7 (2020), 1898. <https://doi.org/10.3390/w12071898>
- [22] Avery Lotz and Ryan Deto. 2025. Flash flood warnings drench the region. <https://www.axios.com/local/pittsburgh/2025/07/24/flash-flood-warnings-allegheeny-county>. <https://www.axios.com/local/pittsburgh/2025/07/24/flash-flood-warnings-allegheeny-county> Accessed: 2025-08-01.
- [23] Ryan Lowe, Yi Wu, Aviv Tamar, Jean Harb, Pieter Abbeel, and Igor Mordatch. 2017. Multi-Agent Actor-Critic for Mixed Cooperative-Competitive Environments. In *Advances in Neural Information Processing Systems (NeurIPS)*, Vol. 30.
- [24] Yecheng Jason Ma, William Liang, Guanzhi Wang, De-An Huang, Osbert Bastani, Dinesh Jayaraman, Yuke Zhu, Linxi Fan, and Anima Anandkumar. 2023. Eureka: Human-Level Reward Design via Coding Large Language Models. *arXiv preprint arXiv:2310.12931* (2023). <https://arxiv.org/abs/2310.12931>
- [25] Riccardo Poli. 2007. *An Analysis of Publications on Particle Swarm Optimisation Applications*. Technical Report CSM-469. Department of Computer Science, University of Essex. <http://citeseerx.ist.psu.edu/viewdoc/download?doi=10.1.1.75.4036&rep=rep1&type=pdf>
- [26] Tabish Rashid, Mikayel Samvelyan, Christian Schroeder, Gregory Farquhar, Jakob Foerster, and Shimon Whiteson. 2018. QMIX: Monotonic Value Function Factorisation for Deep Multi-Agent Reinforcement Learning. In *International Conference on Machine Learning*. PMLR, 4295–4304.
- [27] Craig W. Reynolds. 1987. Flocks, herds and schools: A distributed behavioral model. In *ACM SIGGRAPH Computer Graphics*, Vol. 21. ACM, 25–34. <https://doi.org/10.1145/37402.37406>
- [28] Michael Rubenstein, Alejandro Cornejo, and Radhika Nagpal. 2014. Programmable self-assembly in a thousand-robot swarm. *Science* 345, 6198 (2014), 795–799.
- [29] Adrian Sainz. 2013. \$2.8B damages in 2011 Mississippi River flood. <https://www.mprnews.org/story/2013/02/25/28b-damages-in-2011-mississippi-river-flood>. Accessed: 2025-08-01. Published by MPR News via Associated Press.
- [30] Margaret M. Sugg, Luke Wertis, Sophia C. Ryan, Shannon Green, Devyani Singh, and Jennifer D. Runkle. 2023. Cascading disasters and mental health: The February 2021 winter storm and power crisis in Texas, USA. *Science of The Total Environment* 880 (2023), 163231. <https://doi.org/10.1016/j.scitotenv.2023.163231>
- [31] Sainbayar Sukhbaatar, Arthur Szlam, and Rob Fergus. 2016. Learning Multiagent Communication with Backpropagation. In *Advances in Neural Information Processing Systems (NeurIPS)*, Vol. 29. <https://arxiv.org/abs/1605.07736>
- [32] Ayoub Tahiri, Daniel Che, David Ladeveze, Pascale Chiron, and Bernard Archimède. 2022. Network flow and flood routing model for water resources optimization. *Scientific Reports* 12, 1 (2022), 3937. <https://doi.org/10.1038/s41598-022-07969-4>
- [33] Independent Forensic Team. 2018. *Independent Forensic Team Report: Oroville Spillways Incident*. Technical Report. Dam Safety, Association of State Dam Safety Officials / California Department of Water Resources. Final report (01-05-18 version).
- [34] Mauricio Tec, Guojun Xiong, Haichuan Wang, Francesca Dominici, and Milind Tambe. 2025. Rule-Bottleneck Reinforcement Learning: Joint Explanation and Decision Optimization for Resource Allocation with Language Agents. *arXiv:2502.10732 [cs.LG]* <https://arxiv.org/abs/2502.10732>
- [35] Tamás Vicsek, András Czirók, Eshel Ben-Jacob, Inon Cohen, and Ofer Shochet. 1995. Novel type of phase transition in a system of self-driven particles. *Physical Review Letters* 75, 6 (1995), 1226–1229. <https://doi.org/10.1103/PhysRevLett.75.1226>
- [36] Shen Wang, Ahmad F. Taha, and Ahmed A. Abokifa. 2020. How Effective is Model Predictive Control in Real-Time Water Quality Regulation? State-Space Modeling and Scalable Control. *Water Resources Research* 56, 12 (2020), e2020WR027771. <https://doi.org/10.1029/2020WR027771>
- [37] Guojun Xiong and Milind Tambe. 2025. VORTEX: Aligning Task Utility and Human Preferences through LLM-Guided Reward Shaping. *arXiv:2509.16399 [cs.AI]* <https://arxiv.org/abs/2509.16399>
- [38] Sidney Yakowitz. 1982. Dynamic programming applications in water resources. *Water Resources Research* 18, 4 (1982), 673–696. <https://doi.org/10.1029/WR018i004p0673>
- [39] Chao Yu, Akash Velu, Eugene Vinitzky, Jiaxuan Gao, Yu Wang, Alexandre Bayen, and Yi Wu. 2021. The Surprising Effectiveness of PPO in Cooperative, Multi-Agent Games. *arXiv preprint (2021)*. *arXiv:2103.01955 [cs.LG]* <https://arxiv.org/abs/2103.01955>
- [40] Chao Yu, Akash Velu, Eugene Vinitzky, Jiaxuan Gao, Yu Wang, Alexandre Bayen, and Yi Wu. 2022. The Surprising Effectiveness of PPO in Cooperative Multi-Agent Games. In *Advances in Neural Information Processing Systems*, Vol. 35. 25072–25085.
- [41] Qian Yu, Yanyan Wang, and Na Li. 2022. Extreme Flood Disasters: Comprehensive Impact and Assessment. *Water* 14, 8 (2022), 1211. <https://doi.org/10.3390/w14081211>
- [42] Kaiqing Zhang, Tao Sun, Yunzhe Tao, Sahika Genc, Sunil Mallya, and Tamer Başar. 2020. Robust Multi-Agent Reinforcement Learning with Model Uncertainty. In *Advances in Neural Information Processing Systems (NeurIPS)*. <https://proceedings.neurips.cc/paper/2020/file/774412967f19ea61d448977ad9749078-Paper.pdf>

## A Appendix

This section provides a list of the mathematical symbols and notations used throughout the paper.

### A.1 General System Notation

Symbol	Definition
$\mathcal{G} = (\mathcal{V}, \mathcal{E})$	Directed graph representing the reservoir network
$\mathcal{V}$	Set of reservoir nodes, $\mathcal{V} = \{v_1, v_2, \dots, v_N\}$
$N$	Total number of reservoirs in the network
$\mathcal{E}$	Set of water flow channels, $\mathcal{E} \subseteq \mathcal{V} \times \mathcal{V}$
$t$	Time index
$T$	Planning horizon (final time step)
$\tau$	Communication delay between reservoirs
$H$	Weather forecast horizon length

### A.2 Reservoir State Variables

Symbol	Definition
$\mathbf{s}_i(t)$	State vector of reservoir $i$ at time $t$
$h_i(t)$	Water level (meters) of reservoir $i$ at time $t$
$q_{in,i}(t)$	Aggregate incoming flow to reservoir $i$ at time $t$
$q_{out,i}(t)$	Aggregate outgoing flow from reservoir $i$ at time $t$
$\omega_i(t)$	Local weather conditions vector at reservoir $i$
$d_i(t)$	Time-varying demand at reservoir $i$
$A_i$	Surface area of reservoir $i$
$h_{safe,i}$	Safety threshold water level for reservoir $i$
$h_{min}$	Minimum allowable water level
$h_{max}$	Maximum allowable water level

### A.3 Flow and Transfer Variables

Symbol	Definition
$f_{ij}(t)$	Actual water transfer from reservoir $i$ to $j$ at time $t$
$a_{i \rightarrow k}(t)$	Controlled release from reservoir $i$ to downstream $k$
$q_{ext,i}(t)$	External inflows (rainfall, tributaries) to reservoir $i$
$F_{eco}(t)$	Minimum ecological flow requirements at time $t$
$\mathcal{N}_i^{up}$	Set of upstream neighbors of reservoir $i$
$\mathcal{N}_i^{down}$	Set of downstream neighbors of reservoir $i$
$\mathcal{N}_i$	All neighboring reservoirs, $\mathcal{N}_i = \mathcal{N}_i^{up} \cup \mathcal{N}_i^{down}$

### A.4 Uncertainty and Channel Efficiency

Symbol	Definition
$\alpha_{ij}(t)$	Time-varying channel efficiency between reservoirs $i$ and $j$
$\alpha_{nominal}$	Nominal channel efficiency under normal conditions
$\epsilon$	Minimum channel efficiency threshold (0.1)
$\epsilon_{ij}(t)$	Random fluctuations in water transfer
$Y_{env}(\cdot)$	Weather-induced loss function
$Y_{human}(\cdot)$	Human activity-induced loss function
$\hat{Y}_{human}(t)$	LLM-estimated human-induced variations
$\eta_i(t)$	Measurement noise, $\eta_i(t) \sim \mathcal{N}(0, \sigma_\eta^2)$
$\sigma_{base}$	Base uncertainty level in the system
$\sigma_\eta$	Standard deviation of measurement noise
$\mathcal{T}(t)$	Textual sources (news, regulations, alerts) at time $t$

## A.5 Multi-Objective Functions

Symbol	Definition
$J_{safety}(\pi)$	Safety objective (flood prevention)
$J_{supply}(\pi)$	Supply objective (demand satisfaction)
$J_{ecology}(\pi)$	Ecological objective (environmental flow)
$J_{efficiency}(\pi)$	Efficiency objective (operational cost)
$\mathbf{J}(\pi)$	Vector of all objectives $[J_{safety}, J_{supply}, J_{ecology}, J_{efficiency}]^\top$
$\lambda_{flood,i}$	Flood risk priority weight for populated areas
$c_{op,i}$	Operational cost per unit water released
$a_{max,i}$	Maximum allowable release rate for reservoir $i$
$\mathbb{I}[\cdot]$	Indicator function (1 if true, 0 if false)

## A.6 Policy and Observation Variables

Symbol	Definition
$\pi$	Decentralized policy for reservoir management
$\pi_i$	Local policy for reservoir $i$ , $\pi_i : \mathcal{O}_i \rightarrow \{a_{i \rightarrow k}(t)\}_{k \in \mathcal{N}_i^{down}}$
$\mathcal{O}_i(t)$	Local observation space of reservoir $i$ at time $t$
$\mathbf{s}_j(t - \tau)$	Delayed state information from neighbor $j$
$\omega_{forecast,i}(t:t+H)$	$H$ -hour weather forecast for reservoir $i$

## A.7 Murmuration Coordination Parameters

Symbol	Definition
$\mathcal{L}_{align,i}(t)$	Alignment coordination loss for reservoir $i$
$\mathcal{L}_{sep,i}(t)$	Separation coordination loss for reservoir $i$
$\mathcal{L}_{coh,i}(t)$	Cohesion coordination loss for reservoir $i$
$\mathcal{L}_{total,i}(t)$	Total coordination loss for reservoir $i$
$w_{ij}(t)$	Time-varying coordination weight between $i$ and $j$
$\bar{a}_{ij}(t)$	Average release between reservoirs accounting for delay
$\delta_{ij}$	Geographic distance between reservoirs $i$ and $j$
$\beta_d$	Distance scaling parameter in coordination weights
$\beta_e$	Environmental similarity scaling parameter
$\phi_{sep}(\cdot)$	Separation penalty function
$\rho_i(t)$	Adaptive diversity radius for reservoir $i$
$\rho_{base}$	Base separation threshold
$CV[\cdot]$	Coefficient of variation operator
$\mathcal{P}_i$	Reservoirs in same ecological region as $i$
$\lambda_{eco,i}(t)$	Time-varying ecological coordination weight
$\kappa_{align}, \kappa_{sep}, \kappa_{coh}$	Coordination weights (sum to 1)

## A.8 MARL Architecture Components

Symbol	Definition
$\mathbf{s}_i^{MARL}(t)$	Enhanced state representation for MARL agent $i$
$GNN_\theta(\cdot)$	Graph Neural Network with parameters $\theta$
$LSTM_\phi(\cdot)$	Long Short-Term Memory network with parameters $\phi$
$\mathbf{e}_{ij}$	Edge features $[\bar{a}_{ij}(t), \delta_{ij}]$ between reservoirs
$K$	Historical time window length
$\mathbf{h}_i^{(1)}$	First hidden layer representation
$\mathbf{h}_i^{(2)}$	Enhanced hidden state with murmuration signals
$\xi$	Murmuration influence strength
$MLP(\cdot)$	Multi-layer perceptron
$\nabla_{a_i} \mathcal{L}_{align,i}$	Gradient of alignment loss w.r.t. action $a_i$

## A.9 PPO Training Parameters

Symbol	Definition
$J_i^{\text{PPO}}$	Modified PPO objective for agent $i$
$\mathcal{B}_i$	Experience batch for agent $i$
$r_t(\theta_i)$	Probability ratio $\frac{\pi_{\theta_i}(a_t s_t)}{\pi_{\theta_i^{\text{old}}}(a_t s_t)}$
$\pi_{\theta_i}(\cdot)$	Policy of agent $i$ with parameters $\theta_i$
$\pi_{\theta_i^{\text{old}}}(\cdot)$	Old policy before update
$A_t$	Advantage function at time $t$
$\epsilon$	PPO clipping parameter
$\beta_{\text{mur}}$	Dynamic weight for murmuration penalty

## A.10 LLM and Reward Shaping

Symbol	Definition
$R_i(t)$	Total instantaneous reward for agent $i$
$r_{\text{safety},i}(\cdot)$	Safety component of base reward
$r_{\text{supply},i}(\cdot)$	Supply component of base reward
$r_{\text{eco},i}(\cdot)$	Ecological component of base reward
$R_{\text{shaped},i}(\psi(t))$	LLM-guided contextual reward shaping
$\psi(t)$	LLM-processed control parameters at time $t$
$\text{LLM}(\cdot)$	Large Language Model processing function

## A.11 Mathematical Operators and Distributions

Symbol	Definition
$\mathbb{E}_{\pi}[\cdot]$	Expected value under policy $\pi$
$\mathcal{N}(\mu, \sigma^2)$	Normal distribution with mean $\mu$ , variance $\sigma^2$
$\sim$	"Distributed according to"
$\ \cdot\ _2$	Euclidean (L2) norm
$\ \cdot\ $	General norm (context-dependent)
$ \cdot $	Cardinality of a set or absolute value
$\max(\cdot), \min(\cdot)$	Maximum and minimum functions
$\nabla$	Gradient operator
$\frac{d}{dt}$	Time derivative
$\mathbf{T}$	Matrix/vector transpose
$\in$	"Element of"
$\subseteq$	"Subset of"
$\cup$	Set union

**Note:** All variables with subscript  $i$  refer to reservoir  $i$ , subscript  $j$  refers to neighboring reservoirs. Time dependencies ( $t$ ) are shown when relevant to temporal evolution.

## A.12 Algorithm Pseudocode

This section provides detailed algorithmic descriptions of the key components in MARLIN.

### Algorithm 1: MARLIN Training Algorithm

---

**Require:** Reservoir network  $\mathcal{G} = (\mathcal{V}, \mathcal{E})$ , training data  $\mathcal{D}$ , LLM model, initial weights  $\{\kappa_{\text{align}}, \kappa_{\text{sep}}, \kappa_{\text{coh}}\}$

**Ensure:** Trained policies  $\{\pi_i\}_{i=1}^N$

- 1: Initialize policy networks  $\{\pi_{\theta_i}\}_{i=1}^N$  and value networks  $\{V_{\phi_i}\}_{i=1}^N$
- 2: Initialize LLM processor with RAG knowledge base
- 3: Set default coordination weights:  $\kappa_{\text{align}} = 0.6, \kappa_{\text{sep}} = 0.1, \kappa_{\text{coh}} = 0.3$
- 4: **for** episode  $e = 1, 2, \dots, E$  **do**
- 5:   Reset environment to initial state  $s_0$
- 6:   Initialize experience buffers  $\mathcal{B}_i = \emptyset$  for all agents  $i \in \mathcal{V}$
- 7:   **for** time step  $t = 0, 1, \dots, T - 1$  **do**
- 8:     **for** each reservoir  $i \in \mathcal{V}$  **do**
- 9:      Observe local state
- 10:       $\mathbf{s}_i(t) = [h_i(t), q_{\text{in},i}(t), q_{\text{out},i}(t), \boldsymbol{\omega}_i(t), d_i(t)]^\top$
- 11:      Get neighbor states  $\{\mathbf{s}_j(t - \tau)\}_{j \in \mathcal{N}_i}$  with delay  $\tau$
- 12:      Process with  $\text{GNN}_{\theta}(\{\mathbf{s}_j(t - \tau), \mathbf{e}_{ij}\}_{j \in \mathcal{N}_i})$
- 13:      Extract history with  $\text{LSTM}_{\phi}(\{\mathbf{s}_i(k)\}_{k=t-K}^t)$
- 14:      Construct  $\mathbf{s}_i^{\text{MARL}}(t)$  using Eq. (16)
- 15:     **end for**
- 16:     **if** environmental change detected in  $\mathcal{T}(t)$  **then**
- 17:       Query LLM:  $\psi(t) = \text{LLM}(\mathcal{T}(t))$
- 18:       Update  $(\kappa_{\text{align}}, \kappa_{\text{sep}}, \kappa_{\text{coh}})$  from  $\psi(t)$
- 19:     **end if**
- 20:     **for** each reservoir  $i \in \mathcal{V}$  **do**
- 21:      Compute  $\mathcal{L}_{\text{align},i}(t)$  using Eq. (11)
- 22:      Compute  $\mathcal{L}_{\text{sep},i}(t)$  using Eq. (13)
- 23:      Compute  $\mathcal{L}_{\text{coh},i}(t)$  using Eq. (15)
- 24:      Calculate gradients  $\nabla_{a_i} \mathcal{L}_{\text{align},i}, \nabla_{a_i} \mathcal{L}_{\text{sep},i}, \nabla_{a_i} \mathcal{L}_{\text{coh},i}$
- 25:      Update hidden state:  $\mathbf{h}_i^{(2)} = \mathbf{h}_i^{(1)} + \xi \cdot \text{MLP}([\nabla_{a_i} \mathcal{L}]^\top)$
- 26:      Sample actions:  $\{a_{i \rightarrow k}(t)\}_{k \in \mathcal{N}_i^{\text{down}}} \sim \pi_{\theta_i}(\cdot | \mathbf{s}_i^{\text{MARL}}(t))$
- 27:     **end for**
- 28:     Execute actions, observe  $\{\mathbf{s}_i(t + 1)\}$  and compute  $\{R_i(t)\}$  via Eq. (20)
- 29:     Store  $(\mathbf{s}_i^{\text{MARL}}(t), a_i(t), R_i(t), \mathbf{s}_i^{\text{MARL}}(t + 1))$  in  $\mathcal{B}_i$
- 30:     **end for**
- 31:     **if**  $e \bmod U = 0$  **then**
- 32:       **for** each reservoir  $i \in \mathcal{V}$  **do**
- 33:          Update  $\pi_{\theta_i}$  using PPO objective Eq. (18)
- 34:          Update value function  $V_{\phi_i}$
- 35:       **end for**
- 36:     **end if**
- 37: **end for**
- 38: **return** Trained policies  $\{\pi_{\theta_i}\}_{i=1}^N$

---

**Algorithm 2:** LLM-Guided Reward Shaping

---

**Require:** Context  $\mathcal{T}(t)$ , base rewards  $\{r_{\text{safety},i}, r_{\text{supply},i}, r_{\text{eco},i}\}$ , LLM model

**Ensure:** Shaped rewards  $\{R_i(t)\}$  and weights  $(\kappa_{\text{align}}, \kappa_{\text{sep}}, \kappa_{\text{coh}})$

- 1: Parse textual sources:  
 $\mathcal{T}(t) = \{\text{weather alerts, regulations, news}\}$
- 2: Determine operational mode based on timing:
- 3: **if** Strategic Mode (24h cycle) **then**
- 4:   Prompt LLM with daily context and historical patterns
- 5:   Extract baseline weights:  
     $(\kappa_{\text{align}}, \kappa_{\text{sep}}, \kappa_{\text{coh}}) \leftarrow \text{LLM}(\mathcal{T}(t))$
- 6:   Example: Drought  $\rightarrow (0.6, 0.1, 0.3)$  for conservation
- 7: **else if** Tactical Mode (4h cycle) **then**
- 8:   Query LLM with evolving conditions
- 9:   Adjust weights:  $(\kappa_{\text{align}}, \kappa_{\text{sep}}, \kappa_{\text{coh}}) \leftarrow \text{LLM}(\mathcal{T}(t))$
- 10:   Example: Storm approaching  $\rightarrow (0.2, 0.6, 0.2)$  for diversity
- 11: **else if** Operational Mode (10min emergency) **then**
- 12:   Apply pre-computed emergency weights
- 13:   Set:  $(\kappa_{\text{align}}, \kappa_{\text{sep}}, \kappa_{\text{coh}}) = (0.1, 0.8, 0.1)$
- 14:   Example: Flash flood  $\rightarrow$  maximize independent response
- 15: **end if**
- 16: Extract  $\hat{y}_{\text{human}}(t)$  from LLM output via Eq. (21)
- 17: **for** each reservoir  $i \in \mathcal{V}$  **do**
- 18:   Compute base rewards:  $r_{\text{safety},i}(h_i(t)) + r_{\text{supply},i}(q_{\text{out},i}(t), d_i(t)) + r_{\text{eco},i}(q_{\text{out},i}(t))$
- 19:   Apply LLM shaping:  $R_{\text{shaped},i}(\psi(t))$  based on context
- 20:   Combine:  $R_i(t) = r_{\text{base},i} + R_{\text{shaped},i}(\psi(t))$
- 21: **end for**
- 22: Update channel efficiency via Eq. (22):  
 $\alpha_{ij}(t) \leftarrow \alpha_{\text{nominal}} \cdot [1 - \gamma_{\text{env}} - \hat{y}_{\text{human}}(t)]$
- 23: **return**  $\{R_i(t)\}_{i=1}^N$  and  $(\kappa_{\text{align}}, \kappa_{\text{sep}}, \kappa_{\text{coh}})$

---

## A.13 Detailed Experimental Settings

### A.13.1 Hyperparameter Configuration.

**Algorithm 3:** Murmuration Coordination Computation

---

**Require:** Actions  $\{a_{i \rightarrow k}(t)\}$ , states  $\{s_i(t)\}$ , weights  $(\kappa_{\text{align}}, \kappa_{\text{sep}}, \kappa_{\text{coh}})$

**Ensure:** Total coordination losses  $\{\mathcal{L}_{\text{total},i}(t)\}$

- 1: **for** each reservoir  $i \in \mathcal{V}$  **do**
- 2:   Initialize:  $\mathcal{L}_{\text{align},i} = 0, \mathcal{L}_{\text{sep},i} = 0, \mathcal{L}_{\text{coh},i} = 0$
- 3:   // **Alignment Rule - Encourage coordinated releases**
- 4:   **for** each neighbor  $j \in \mathcal{N}_i^{\text{up}} \cup \mathcal{N}_i^{\text{down}}$  **do**
- 5:     Compute weight using Eq. (12):
- 6:      $w_{ij}(t) = \frac{\exp(-\beta_d \delta_{ij} - \beta_e \|\omega_i(t) - \omega_j(t)\|_2)}{\sum_{k \in \mathcal{N}_i} \exp(-\beta_d \delta_{ik} - \beta_e \|\omega_i(t) - \omega_k(t)\|_2)}$
- 7:     Compute average:  
     $\bar{a}_{ij}(t) = \frac{1}{2} [\sum_k a_{i \rightarrow k}(t) + \sum_k a_{j \rightarrow k}(t - \tau)]$
- 8:     Update:  
     $\mathcal{L}_{\text{align},i} \leftarrow \mathcal{L}_{\text{align},i} + w_{ij}(t) \cdot \|\sum_k a_{i \rightarrow k}(t) - \bar{a}_{ij}(t)\|^2$
- 9:   **end for**
- 10:   // **Separation Rule - Maintain strategic diversity**
- 11:   Compute adaptive radius using Eq. (14):
- 12:    $\rho_i(t) = \rho_{\text{base}} \cdot (1 + \text{CV}[\{h_j(t - \tau)\}_{j \in \mathcal{N}_i}])$
- 13:   **for** each neighbor  $j \in \mathcal{N}_i$  **do**
- 14:      $\mathcal{L}_{\text{sep},i} \leftarrow \mathcal{L}_{\text{sep},i} + \phi_{\text{sep}} (\|\sum_k a_{i \rightarrow k}(t) - \sum_k a_{j \rightarrow k}(t - \tau)\|_2; \rho_i(t))$
- 15:   **end for**
- 16:   // **Cohesion Rule - Meet ecological requirements**
- 17:   Identify ecological region:  $\mathcal{P}_i \subseteq \mathcal{V}$
- 18:   Compute actual flow:  $Q_{\text{actual}} = \sum_{j \in \mathcal{P}_i} q_{\text{out},j}(t - \tau)$
- 19:    $\mathcal{L}_{\text{coh},i} = \lambda_{\text{eco},i}(t) \cdot \|Q_{\text{actual}} - \frac{F_{\text{eco}}(t)}{|\mathcal{P}_i|}\|^2$
- 20:   // **Total Loss with Dynamic Weights**
- 21:    $\mathcal{L}_{\text{total},i}(t) = \kappa_{\text{align}} \cdot \mathcal{L}_{\text{align},i} + \kappa_{\text{sep}} \cdot \mathcal{L}_{\text{sep},i} + \kappa_{\text{coh}} \cdot \mathcal{L}_{\text{coh},i}$
- 22: **end for**
- 23: **return**  $\{\mathcal{L}_{\text{total},i}(t)\}_{i=1}^N$

---

Component	Parameter	Value
PPO Training	Learning rate (policy)	$3 \times 10^{-4}$
	Learning rate (value)	$1 \times 10^{-3}$
	Clipping parameter $\epsilon$	0.2
	GAE parameter $\lambda$	0.95
	Discount factor $\gamma$	0.99
	Batch size	512
	Update epochs	10
	Update frequency $U$	4 episodes
Network Architecture	GNN hidden dimensions	[64, 128, 64]
	LSTM hidden size	128
	Policy network layers	[256, 256, 128]
	Value network layers	[256, 256, 1]
	Activation function	ReLU
	Dropout rate	0.1
Murmuration Parameters	Distance scaling $\beta_d$	0.1
	Environmental scaling $\beta_e$	0.5
	Base separation radius $\rho_{\text{base}}$	0.3
	Murmuration influence $\xi$	0.1
	Coordination weight $\beta_{\text{mur}}$	0.05
	Default $\kappa_{\text{align}}$	0.6
	Default $\kappa_{\text{sep}}$	0.1
	Default $\kappa_{\text{coh}}$	0.3
LLM Configuration	Model	Gemini-1.5-Pro
	Context window	1 million tokens
	Temperature	0.3
	Max output tokens	2048
	Strategic update cycle	24 hours
	Tactical update cycle	4 hours
	Operational response	10 minutes

### A.13.2 Hardware and Computational Details.

Component	Specification
GPU	NVIDIA RTX 4090 (24GB) × 2
Memory	64GB DDR5
Framework	PyTorch 2.2, CUDA 11.8
Data parallelism	1.8× speedup
Processing time (10k nodes)	1,847.3ms
Memory footprint (10k nodes)	21.67GB

### A.13.3 Baseline Implementation.

Method	Configuration	Complexity
MADDPG	Centralized critic, decentralized actors	$O(N^2)$
QMX	Value decomposition, monotonic mixing	$O(N^2)$
MAPPO	Same PPO settings as MARLIN	$O(N^2)$
MPC-Centralized	Horizon: 24h, Solver: IPOPT	$O(N^3)$
<b>MARLIN (Ours)</b>	Murmuration + MARL + LLM	$O(N)$

## A.14 LLM Prompt Templates and Examples

### A.14.1 Strategic Planning Template (24-hour cycle).

#### Strategic Planning Prompt Template

**SYSTEM:** You are managing a network of  $N$  interconnected reservoirs.

**CONTEXT:**

- Current date and time: {timestamp}
- Network status: {reservoir\_levels}
- Weather forecast: {weather\_data}
- Demand forecast: {demand\_patterns}

**CONSTRAINTS:**

- Regulatory: {regulations}
- Environmental: Minimum flow  $F_{eco}(t) = \{eco\_flow\}$  cfs
- Operational:  $h_{min} \leq h_i(t) \leq h_{max}$

**TASK:** Generate coordination weights  $(\kappa_{align}, \kappa_{sep}, \kappa_{coh})$  where  $\sum \kappa = 1$ .

**OUTPUT FORMAT:**

weights: {align: float, sep: float, coh: float}  
 gamma\_human: float  
 rationale: string

### A.14.2 Tactical Adjustment Template (4-hour cycle).

#### Tactical Adjustment Prompt Template

**CURRENT WEIGHTS:**  $(\kappa_{align}, \kappa_{sep}, \kappa_{coh}) =$   
 {current\_weights}

**EVOLVING CONDITIONS:**

- Real-time sensor data: {sensor\_updates}
- Updated forecast: {forecast\_changes}
- System performance: {performance\_metrics}

**TASK:** Adjust coordination weights based on evolving conditions.

**ADJUSTMENT RULES:**

- If uncertainty increases → increase  $\kappa_{sep}$
- If emergency detected → increase  $\kappa_{align}$
- If ecological stress → increase  $\kappa_{coh}$

### A.14.3 Emergency Response Template (10-minute cycle).

#### Emergency Response Template

**EMERGENCY TYPE:** {emergency\_classification}

**PRE-COMPUTED RESPONSES:**

- **Flood:**  $(\kappa_{align}, \kappa_{sep}, \kappa_{coh}) = (0.1, 0.8, 0.1)$
- **Drought:**  $(\kappa_{align}, \kappa_{sep}, \kappa_{coh}) = (0.8, 0.1, 0.1)$
- **Contamination:**  $(\kappa_{align}, \kappa_{sep}, \kappa_{coh}) = (0.2, 0.7, 0.1)$

**IMMEDIATE ACTION:** Apply pre-computed weights without LLM query to minimize latency.

### A.14.4 Example LLM Interactions.

*Example 1: Drought Response.*

**Input:** California Central Valley, March 2024, Snowpack: 32%, Agricultural demand: High

**LLM Output:**

```
{
  "weights": {"align": 0.7, "sep": 0.1, "coh": 0.2},
  "gamma_human": 0.15,
  "rationale": "Severe drought requires tight coordination
                (high align) to maximize conservation. Low
                separation prevents water waste. Moderate
                cohesion maintains minimum ecological flows."
}
```

### Example 2: Atmospheric River.

**Input:** Pacific Northwest, November 2024, Precipitation: 200% normal, Reservoirs: 85-92% full

**LLM Output:**

```
{
  "weights": {"align": 0.4, "sep": 0.4, "coh": 0.2},
  "gamma_human": 0.05,
  "rationale": "Flood risk requires diverse strategies (high
                sep) allowing some reservoirs to release
                aggressively while others hold capacity.
                Moderate alignment for coordinated timing."
}
```

#### A.14.5 Performance Analysis of LLM Integration.

Metric	Without LLM	With LLM
Uncertainty handling	Baseline	+23%
Flood response time	12.8 hours	3.7 hours (-68%)
Regional water balance	Baseline	+42%
Demand satisfaction (drought)	67.8%	94.3%
Flood prevention rate	71.2%	97.1%
LLM latency (average)	-	0.4s
LLM latency (99th percentile)	-	2.3s
API cost (per month)	\$0	\$15,000*

\*Expected to decrease with model efficiency improvements

#### A.14.6 Data Preprocessing and Feature Engineering.

Processing Step	Details
Normalization	Min-max scaling to [0, 1] for water levels
Weather features	Z-score normalization
Temporal smoothing	3-hour moving average
Missing data	Linear interpolation for gaps < 6 hours
Feature extraction	Hour, day, month, season indicators
Lag features	1, 6, 12, 24-hour lagged values
Rolling statistics	7-day and 30-day means/std

#### A.14.7 Evaluation Protocol.

Aspect	Configuration
Training data	2019-2023 (43,800 timesteps)
Validation data	Jan-Jun 2024 (4,380 timesteps)
Test data	Jul-Dec 2024 (4,380 timesteps)
Cross-validation	5-fold temporal
Random seeds	5 independent runs
Statistical test	Wilcoxon signed-rank
Confidence intervals	95% via bootstrap (1000 samples)